

MIROSŁAWA BUKOWSKA *

THE INFLUENCE OF STRAIN RATE ON INDICES OF ROCK BUMP SUSCEPTIBILITY

WPŁYW PRĘDKOŚCI ODKSZTAŁCENIA SKAŁ NA WSKAŹNIKI SKŁONNOŚCI SKAŁ DO TĄPAŃ

The indexes of rock susceptibility to bumps, which can be determined from uniaxial compression of rock samples in a stiff testing machine have been determined. Experiments have been carried out at kinematic control with longitudinal strain rate ranging between 10^{-4} to 10^{-1} s^{-1} . The results have been obtained in the form of a complete stress-strain characteristic. On this basis indexes of rock susceptibility to bumps have been defined. The stress, strain, stress-strain and energy indexes have been determined. Attention has been paid to the indexes defined from the pre-critical part of the stress-strain characteristic as well as the indexes defined from the pre- and post-critical parts of the characteristic.

The influence of strain rate on the indexes of rock susceptibility to bumps for all kinds of Carboniferous rock occurring in the Upper Silesian Coal Basin has been analysed with respect to the whole population of rock samples.

The obtained results have been referred to the bump prevention measures in two extreme cases: a weak seam under a strong roof or a strong seam under a weak roof.

Key words: stress strain characteristics, pre- and post-critical rock properties, strain rate, bump prevention.

W pracy określono wskaźniki skłonności skał do tąpań, które można uzyskać na podstawie badań jednoosiowego ściskania próbek skalnych w sztywnej maszynie wytrzymałościowej.

Badania eksperymentalne prowadzono w sztywnej maszynie wytrzymałościowej MTS-810 przy wymuszeniu kinematycznym za pomocą prędkości odkształcenia podłużnego w zakresie prędkości odkształcenia 10^{-4} – 10^{-1} s^{-1} (Bukowska, 1996). W badaniach uwzględniono wszystkie rodzaje skał karbońskich formacji węglonośnej Górnego Śląska Zagłębia Węglowego: zlepieńce, piaskowce, mułowce, ilowce, węgle. Dla każdego rodzaju skał przebadano po kilkadesiąt próbek laboratoryjnych (tablica 1). Wyniki badań

* GŁÓWNY INSTYTUT GÓRNICTWA, 40-166 KATOWICE, PL. GWARKÓW 1

uzyskiwano z wykresu komputerowego w postaci całkowej charakterystyki naprężenioowo-odkształceniowej, na podstawie której określano wskaźniki skłonności skał do tąpań. Wyróżniono wskaźniki naprężeniowe, odkształceniowe, naprężeniowo-odkształceniowe i energetyczne (wzory: 4.1–4.6).

Dla określenia wpływu prędkości odkształcenia skały na wielkości charakteryzujące wrażliwości skał do tąpań i wskaźniki skłonności skał do tąpań zastosowano analizę statystyczną, przy uwzględnieniu całej populacji próbek (538 próbek — tab. 1). Dla każdej zależności $y = f(\dot{\varepsilon})$ i dla każdej próbki skalnej określono współczynniki korelacji. W przypadku gdy była możliwość grupowania próbek skalnych danego rodzaju skał, tzn. gdy korelacja badanej zależności $y = f(\dot{\varepsilon})$ dla grupy próbek skalnych była istotna na przyjętym poziomie prawdopodobieństwa 0,05, określano dla całej grupy danego rodzaju jedno równanie regresji. W przeciwnym przypadku podawano równania regresji dla poszczególnych zależności dla każdej próbki oddzielnie.

Otrzymane równania regresji przedstawiają zależności badanego parametru od prędkości odkształcenia skały (rys. 5.1–5.6).

Analiza statystyczna wykazała, że niektóre parametry wykazują zależności od prędkości odkształcenia tylko dla pewnych typów skał.

Istotnym wynikiem analizy statystycznej jest wykazanie, że wskaźniki skłonności skał do tąpań, określone na podstawie przedkrytycznej części charakterystyki naprężenioowo-odkształceniowej: wskaźnik potencjalnej tąpliwości K , energetyczny wskaźnik skłonności do tąpań na granicy wytrzymałości W_{ET} oraz wskaźnik zagrożenia tapaniami W_{ZT} , nie zależą od prędkości odkształcenia skał w badanym zakresie $10^{-4} – 10^{-1} \text{ s}^{-1}$.

Zwróciło uwagę na wskaźniki skłonności skał do tąpań, które zależą od prędkości odkształcienia: wskaźnik potencjalnej energii sprężystej PES, wskaźnik dynamiki rozpadu λ i wskaźnik osłabienia tąpienia W_{OT} . Wskaźnik potencjalnej energii sprężystej wykazuje wzrost wraz ze wzrostem prędkości odkształcenia dla wszystkich badanych typów litologicznych skał. W przypadku piaskowców (rys. 6.1 a) i węgli występuje wyraźne zróżnicowanie wartości PES dla skał pochodzących z różnych kopalń. Natomiast ilowce, mułowce i zlepieńce wykazują jednakowe zmiany dla wszystkich próbek, bez względu na miejsce pobrania (rys. 6.1 b). Wskaźnik dynamiki rozpadu maleje wraz ze wzrostem prędkości odkształcenia dla węgli, ilowów i mułowców, przy czym występujące zależności są jednakowe dla wszystkich próbek tego samego typu litologicznego skały (rys. 6.2). Wskaźnik osłabienia tąpienia zależy od prędkości odkształcenia skały tylko dla mułowców i węgla, wykazując analogiczne zmiany dla całego typu litologicznego skały (rys. 6.3).

Do wskaźników skłonności skał do tąpań zaliczano również naprężenie krytyczne (doraźna wytrzymałość na ściskanie), jako najbardziej charakterystyczną własność skał, którą można określić w warunkach kopalnianych.

Dla globalnego przedstawienia wyników badań skonstruowano trójwymiarowy wykres warstwowy, na którym pokazano zmianę wartości poszczególnych energii właściwych wraz ze wzrostem prędkości odkształcenia. Dla przykładu załączono histogramy dla węgli (rys. 7.1) i dla mułowców (rys. 7.2), gdyż pozostałe typy skał wykazują podobne tendencje zmian. Trójwymiarowe histogramy obrazują nie tylko wpływ prędkości odkształcenia na badane energie, ale również przedstawiają względne wartości poszczególnych energii w stosunku do energii całkowitej.

Na analogicznych histogramach przedstawiono wskaźniki skłonności skał do tąpań dla węgli (rys. 7.3) i dla mułowców (rys. 7.4). Wskaźnik σ_{kr} i PES wyraźnie wzrastają, natomiast wskaźnik λ i W_{OT} ulegają zmniejszeniu wraz ze wzrostem prędkości odkształcenia skały, jednakże szybkość zmian poszczególnych wskaźników zależy od rodzaju skały.

Wyniki badań odniesiono do zagadnień profilaktyki tapaniowej w dwóch skrajnych przypadkach: zalegania słabego pokładu węgla pod mocnym stropem lub mocnego pokładu węgla pod słabym stropem.

We wnioskach zestawiono wyniki badań. Końcowym wnioskiem jest stwierdzenie, że zapobieganie tąpaniom wymaga analizy poszczególnych przypadków zalegania układu: pokład-strop, a następnie stosowania odpowiedniego kierowania zarówno postępu frontu eksploatacyjnego dla wywołania odpowiedniej prędkości odkształcenia skał, jak również kontroli stropu dla zmniejszenia magazynowanej energii przez wymuszone zawały lub nawilżanie skał stropowych.

Słowa kluczowe: charakterystyka naprężeniowo-odkształceniowa, przed- i pokrytyczne własności skał, prędkość odkształcenia, profilaktyka tąpaniowa.

1. Introduction

The prediction of bumps is very difficult as this phenomenon depends on many factors: natural geological conditions (lithology, tectonics), geomechanical conditions (distribution of stresses around workings), on mining method (impact machines or blasting) and also on the stress-strain properties of rocks. These properties are determined in lab conditions on compact rock samples and then adapted to rock masses with regard to the rock structural softening caused by natural conditions.

The susceptibility of rocks to bumps had been determined on the basis of a few parameters defined from stress-strain characteristics in the so-called „soft” testing machines where only the increasing part of the characteristics describing the pre-critical rock properties is obtained. Various criteria of rock susceptibility to bumps resulted from the laboratory analyses. Recently, these criteria have also covered the post-critical rock properties obtained from the decreasing part of the characteristic registered in the stiff testing machines. With the stiff testing machines it is possible not only to acquire the complete stress-strain characteristic, but also to make tests with a constant strain rate.

In the paper the measurement material obtained from tests in a uniaxial state of stress for the basis type of Carboniferous carbonous rocks of the Upper Silesian Coal Basin, i.e. conglomerates, sandstones, mudstones, siltstones and coals are given. The stress-strain and energy parameters have been determined for the following strain rates: 1×10^{-4} , 2×10^{-3} , 2×10^{-2} , 2×10^{-1} , s^{-1} .

Based on the experimental results, the analysis of the influence of the rock strain rate on the parameters characterising the rock susceptibility to bumps has been carried out, in that:

- index of potential bumping,
- index of potential elastic energy,
- index of rock susceptibility to bumps at strength limit,
- index of bump hazard,
- index of bump softening,
- index of dynamic failure.

2. Experimental

The tests of rock destruction process were carried out in a stiff testing machine MTS-810 with a possibility of servo-control. The control parameter of the experimental was the longitudinal strain rate.

The experiments have been performed for five types of sedimentary rocks of the productive Carboniferous in the Upper Silesian Coal Basin. Rock samples were taken from the strata in the regions threatened and non-threatened with bumps (Table 1).

TABLE 1
Type of rocks and place of sampling

Type of rocks	Name of mine	Place of sampling	Depth of deposition [m]	Bump hazard to classification	Number of samples
conglomerate	Niwka-Modrzejów Knurów	seam roof 510 seam roof 417/1	640 850	+-	16 19
sandstone	Staszic	seam roof 352	530	-	25
	Grodziec	seam roof 816	550	-	21
	Piast	seam roof 207	600	+	19
	Knurów	seam roof 402/2	850	-	23
	Pokój	seam roof 504	700	+	26
mudstone	Jan Kanty	seam roof 334	100—350	-	30
	Pokój	seam roof 510	800	+	29
	Krupiński	seam roof 340	820	-	26
	Anna	seam roof 713/1—2	820	+	18
siltstone	Grodziec	seam roof 816	550	-	17
	Śląsk	seam roof 416	650	+	16
	Śląsk	seam floor 416	660	+	15
	Śląsk	seam roof 414	700	+	17
	Krupiński	seam roof 340	820	-	18
coal	Knurów	seam 402/2	850	-	23
	Czeczott	seam 209/1	600	+	27
	Śląsk	seam 416	650	+	19
	Ziemowit	seam 209	670	+	21
	Rozbark	seam 507/510	700	+	23
	Nowy Wirek	seam 502	765	+	20
	Niwka-Modrzejów	seam 620	170—300	-	20
	Grodziec	seam 816	550	-	24
	Niwka-Modrzejów	seam 510	640	+	26

On the whole, 538 samples were tested: 34 conglomerate samples, 114 sandstone samples, 103 mudstone samples, 83 siltstone samples, 203 coal samples.

In laboratory tests, the cubic rock samples of 50 mm side were used. They were tested in a uniaxial state of stress according to the standard PN-G-04303. The direction of the acting force was perpendicular to the lamination.

The tests carried out in a stiff testing machine at a uniaxial state of stress, were controlled by means of longitudinal strains of rock samples measured by the displacement of the piston. The experiments were performed for different strain rates: 1×10^{-4} , 2×10^{-3} , 2×10^{-2} , 2×10^{-1} , s^{-1} . For each strain rate 5 to 7 laboratory samples of different type of rocks were tested.

3. Stress-strain characteristic

With the use of stiff testing machines it was possible to obtain complete stress-strain characteristics having the pre-critical (increasing) and post-critical (decreasing) parts (Fig. 3.1) (Wawersik and Fairhurst, 1970; Filcek, 1986; Majcherczyk, 1989).

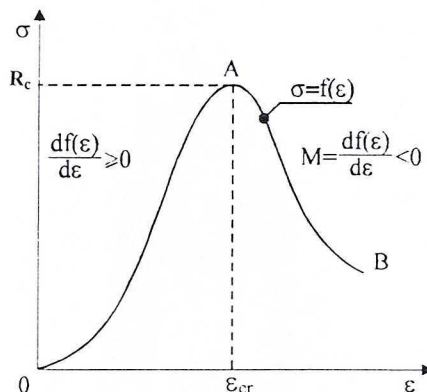


Fig. 3.1. Stress-strain curve — stiff testing machine (Wawersik, Fairhurst, 1970)

The stress-strain characteristic acquired from a uniaxial compression of rock samples in a stiff testing machine shows the process of rock destruction in the pre-critical state for a compact rock (the increase of strain is accompanied by the increase of rock strength) and in the post-critical state when the rock is destroyed (the increase of strain is accompanied by the decrease of rock strength).

3.1. Determination of stress-strain parameters

Rock properties in the pre- and post-critical state were obtained from the complete stress-strain characteristic. From the increasing part of the characteristic the modulus of elasticity E (as a tangent of angle of inclination of tangent to the increasing part of the characteristic in the range of elastic strains) and the critical stress σ_{cr} (compressive strength) were determined. From the decreasing part of the characteristic the post-critical parameters, i.e. drop (softening) modulus M (as

a tangent of angle of inclination of tangent to the decreasing part of the stress-strain characteristic) and residual stress σ_{res} (residual strength to compression) were measured. It should be stressed that the determination of the post-critical parameters is both difficult and subjective. Especially, when defining the modulus M , even a small difference in the post-critical strain value causes a significant difference in the value of the modulus. The elastic ϵ_{el} , critical ϵ_{cr} and total ϵ strains were determined for the corresponding stresses as well.

The characteristic stress-strain parameters are presented in Fig. 3.2.

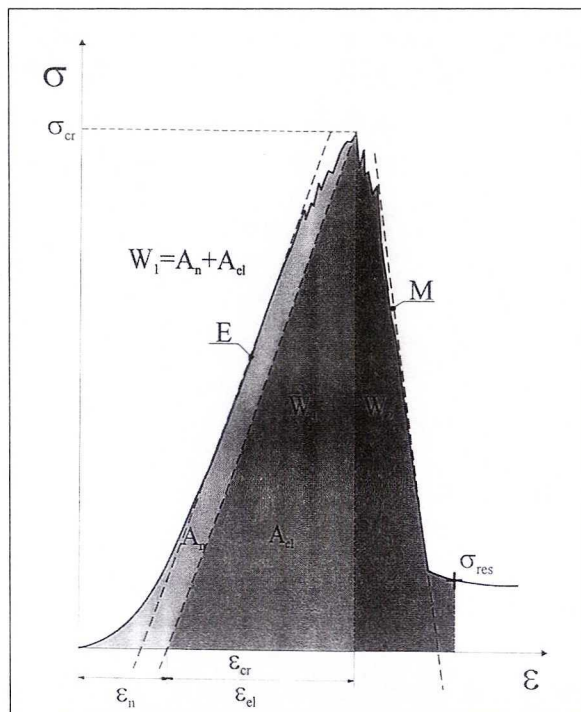


Fig. 3.2. Characteristic of stress-strain parameters and specific energies of longitudinal strain

3.2. Determination of the specific energy of longitudinal strain in samples

The following specific energies have been determined from the stress-strain characteristic: energy of elastic strain A_{el} and energy of non-reversible strain A_n at strength limit as well as energy of post-critical strain W_2 . The area enclosed between the characteristic and the axial of strain defines the specific energy of longitudinal strain of a sample W . This area has been divided into the area under the increasing part W_1 and under the decreasing part W_2 of the characteristic. Then, the areas corresponding to the elastic A_{el} and non-reversible strain A_n at stress limit have been

separated within the area under the increasing part of the characteristic. The introduced division of area between the stress characteristic and the strain axis corresponds to the division of energy into energy necessary to achieve the strength limit W_1 (encompassing the energy of elastic and non-reversible strains at strength limit) and post-critical energy of sample destruction W_2 (Fig. 3.2) (Gustkiewicz, 1987).

3.3. Kinetic energy for rocks having elasto/plastic with softening properties

Kinetic energy determines the character of rock sample failure. To define the kinetic energy of the destroyed rock, the energy balance equation is used. There the energies of elastic strain and of non-reversible strain in the pre- and post-critical stress-strain characteristic are taken into account. According to Heasley (1991), the total energy of strain for the stress-strain characteristic of coals with elasto/plastic with softening properties can be divided into recoverable energy of strain and dissipated energy, being a sum of elastic energy and post-critical energy of rock destruction. The way in which individual energies are determined, has been presented in Fig. 3.3.

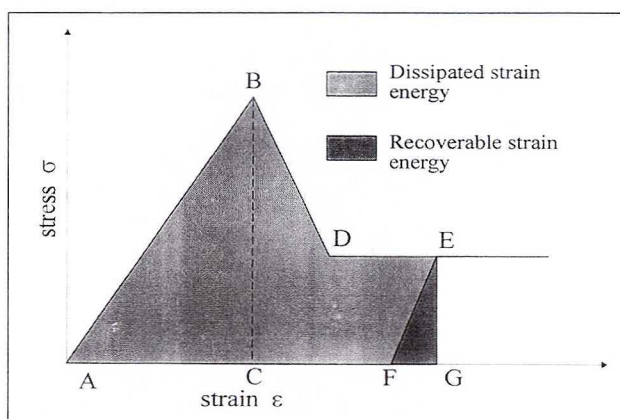


Fig. 3.3. Scheme of division of total strain energy (Heasley, 1991)

Based on the model assumed by Heasley, only the value of recovered energy of strain can be transformed into kinetic energy (Heasley, 1991).

Kinetic energy of rock samples analysed in a stiff testing machine can be defined from the equation:

$$E_k = A_{el} - W_2 + W_3 \quad (3.1)$$

where: A_{el} defines elastic energy accumulated in a rock sample, W_2 is the strain energy in the post-critical part of the stress-strain characteristic, and W_3 shows the recoverable energy of strain.

4. Determining the indexes of susceptibility of rocks to bumps

The indexes of susceptibility of rocks to bumps have been determined on the basis of complete stress-strain characteristics and specific energies within the individual ranges of longitudinal strain of rock samples. They are:

- *index of potential bumping K* (Bicz, 1962) expressed by the elastic strain ε_{el} to critical strain ε_{cr} ratio:

$$K = (\varepsilon_{el}/\varepsilon_{cr}) 100\% \quad (4.1)$$

- *index of dynamic failure λ* (Minh, 1989) expressed by the drop modulus M to the modulus of longitudinal elasticity E ratio:

$$\lambda = M/E. \quad (4.2)$$

The use of the index is justified when the part of the destroyed sample can be approximated through a linear relation.

- *index of potential elastic energy PES* (Smołka, 1988) determined from the formula:

$$PES = R_c^2/2E. \quad (4.3)$$

This index accounts for the accumulation of energy, corresponding to the compressive strength R_c for the linear stress-strain dependence with the Young's modulus E .

- *energy index of susceptibility of rocks to bumps at strength limit W_{ET}'* , (Gustkiewicz et al., 1987) defined by the elastic energy to non-reversible energy at strength limit ratio:

$$W_{ET}' = A_{el}/A_n \quad (4.4)$$

- *index of bump hazard W_{ZT}* also called index of brittleness (Gustkiewicz et al., 1987) calculated from the formula:

$$W_{ZT} = A_{el}/W_1, \quad (4.5)$$

where: A_{el} — energy of elastic strains, W_1 — energy of longitudinal strain in the pre-critical part.

The closer is the index W_{ZT} to unity, the more rapid the rock failure.

- *index of bump softening W_{OT}* (Krzysztoń, 1989) expressed by the elastic energy A_{el} to the energy of post-critical failure W_2 ratio:

$$W_{OT} = A_{el}/W_2, \quad (4.6)$$

This index depends on the value of energy necessary for stable destruction of a sample, occurring in the post-critical part of the stress-strain characteristic. The bigger the share of elastic energies in the energy of post-critical strain of a sample the lesser the bump hazard.

5. Analysis of investigation results with regard to the strain rate of a rock sample

The application in tests of different strain rates made it possible to analyse the influence of strain rates on stress, strain, and specific energies as well as on indexes defining the susceptibility of rock to bumps (for different rock samples) (Bukowska, 1994, 1996).

The statistical analysis was carried out on the whole population of data obtained from the investigation of each sample from a 538 set of samples (Table 1).

The correlation coefficients were defined for each dependence $y = f(\dot{\varepsilon})$ and for each rock sample. Whenever it was possible to group the rock samples according to the rock type, e.g. when the correlation of a given dependence $y = f(\dot{\varepsilon})$ for rock samples was significant at the assumed significance level 0.05, one regression equation was defined for the whole group of rocks.

Otherwise, the regression equation was used for the individual dependences $y = f(\dot{\varepsilon})$ for each rock sample separately. The dependences between the stress, strain, bump susceptibility indexes and the strain rate in the interval 10^{-4} to 10^{-1} s^{-1} can be best approximated by a power function (the highest correlation coefficient, the lowest standard deviation), and in certain cases by a linear function. The above dependences were presented graphically in the form of the regression curve and the confidence interval at the level $1 - \alpha = 0.95$ and $1 - \alpha = 0.99$, i.e. areas containing values of the observed random variables with the probability equal to 0.95 and 0.99, respectively. The confidence interval for regression is limited by the so-called confidence curves (broken line in the figures).

To better understand the distribution of a given parameter for the strain rates interval 10^{-4} to 10^{-1} s^{-1} , the dependences of stress, strain and bump susceptibility parameters were given as functions of the logarithm of strain rate (see examples in Figures 5.1—5.6).

5.1. Analysis of stress-strain parameters

The growth of critical stress σ_{cr} with the increasing strain rate was observed for rocks surrounding coal seams and coals coming from various depths in the bumping and non-bumping regions. The critical stress values as a function of strain rate for all rock types change according to the power function $y = ax^b$. The graph in Fig. 5.1 represents the function $\sigma_{cr} = f(\log \dot{\varepsilon})$ for siltstones from different collieries and different lithostratigraphic complexes of the Carboniferous. This could be done thanks to the possibility of determining one regression equation for the whole lithological type.

The influence of strain rate on the elasticity modulus E depends on rock properties (brittle rock or viscous-elastic rock). For certain rocks (conglomerates, sandstones and coals) no influence of strain rate on elasticity modulus has been observed. For mudstones (having a considerable clayey content, and thus possessing viscous-elastic properties) and for siltstones (Fig. 5.2), the influence of strain rate on elasticity modulus has been reported.

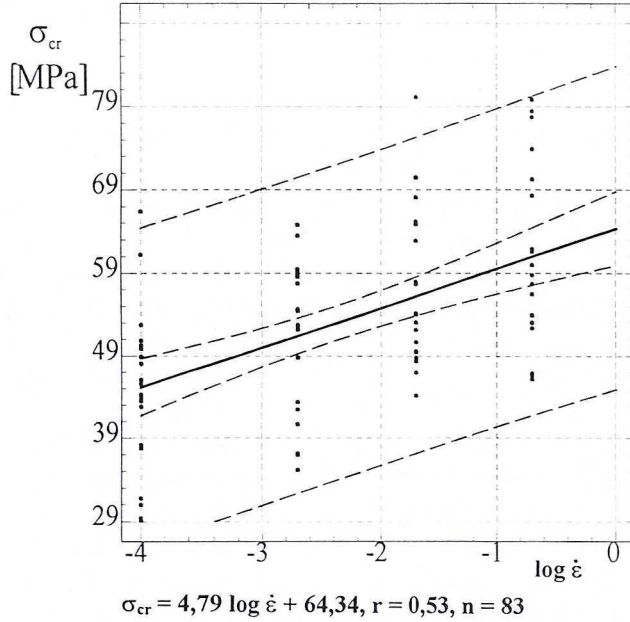


Fig. 5.1. Critical stress as a function of log strain rate for siltstones

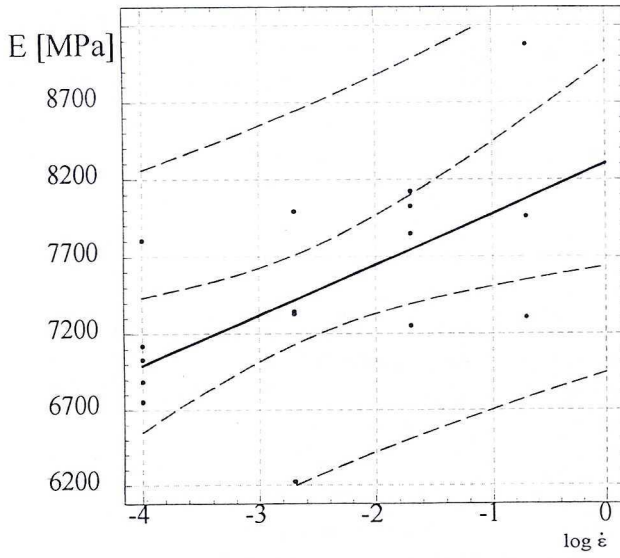


Fig. 5.2. Young's modulus as a function of log strain rate for a siltstone sample

The post-critical part of the stress-strain characteristic has been described by the drop (softening) modulus. It is widely known that opinions on the change of the drop with the change of strain rate are often different. According to some of them, the

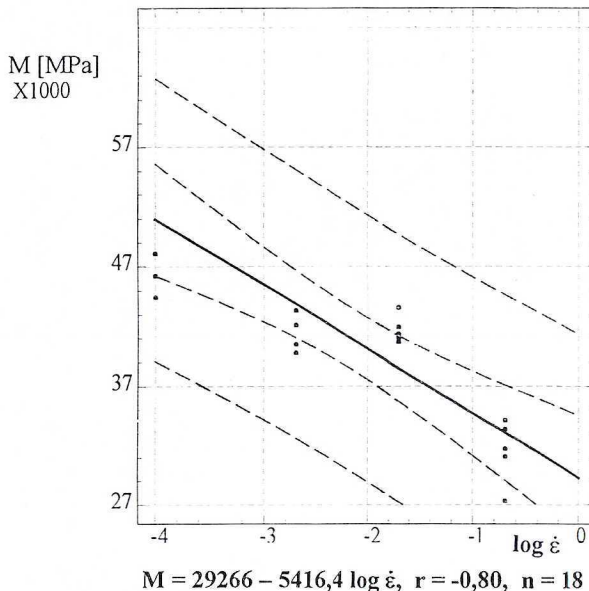


Fig. 5.3. Drop modulus (modulus of softening) as a function of log strain rate for a mudstone sample

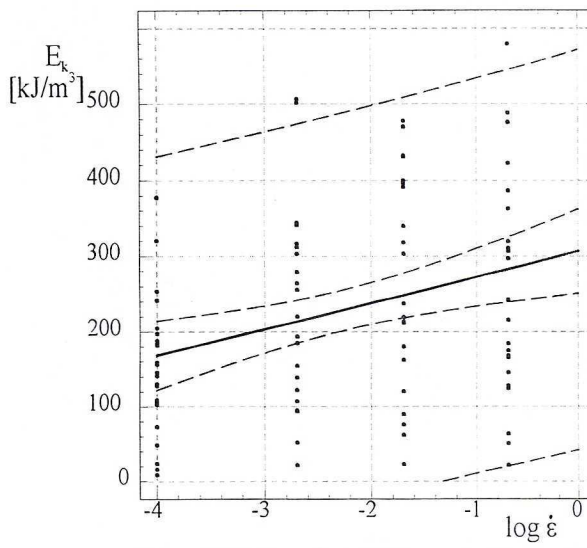
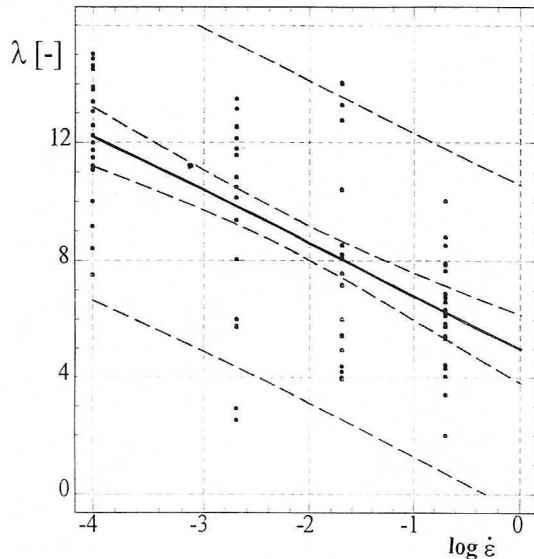


Fig. 5.4. Kinetic energy as a function of log strain rate for a dull coal sample

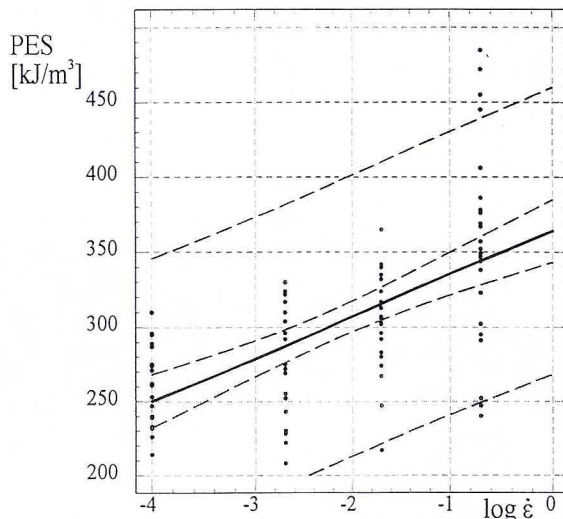
increase of strain rate causes the increase of drop modulus (Bieniawski, 1970) or the decrease of drop modulus (Peng, 1973).

The following has been found for the analysed rocks (Bukowska, 1996) (Table 1):



$$\lambda = 4,97 - 1,81 \log \dot{\epsilon}, r = -0,63, n = 91$$

Fig. 5.5. Index of dynamic failure as a log function of strain rate for semi-bright coals



$$PES = 28,5 \log \dot{\epsilon} + 364, r = 0,61, n = 103$$

Fig. 5.6. Index of potential elastic energy as a log function of strain rate for mudstones

- drop modulus for conglomerates, sandstones and dull coals does not depend on the strain rate,
- drop modulus or mudstones (Fig. 5.3) decreases with the increasing strain rate in the range 10^{-4} to 10^{-1} s^{-1} ,

- drop modulus for bright coal (compression strength 14 to 20 MPa) increases with the increase of strain rate according to a power relation,
- drop modulus for semi-bright coals (compression strength 20 to 40 MPa) decreases with the increase of strain rate.

5.2. Analysis of specific energy of longitudinal strain

Specific energy of longitudinal strain has been determined from the graphs $\sigma - \varepsilon$, distinguishing the energy of pre-critical strain of sample W_1 , being a sum of energy of elastic strain A_{el} and non-reversible strain A_n and energy of post-critical strain (Gustkiewicz et al., 1987; Krzysztoń, 1989, 1992; Krzysztoń, Sanetra, 1994).

The energy of specific strain W_1 at strength limit increases with the strain rate for the investigated five Carboniferous rock types in the analysed range of strain rates 10^{-4} to 10^{-1} s^{-1} . For rocks surrounding coal seams and for coals the dependence of specific strain energy W_1 on strain rate assumes the form of a power function and in a semi-logarithmic system in the form of a linear function.

The energy of elastic strain A_{el} is strongly influenced by strain rate in the range 10^{-4} to 10^{-1} s^{-1} . The dependence has the form of a power regression with positive correlation coefficients.

The energy of non-reversible strain at strength limit A_n does not exhibit regular changes with the increase of strain rates for all analysed rock samples; for sandstones it does not depend on the strain rate. The dependence $A_n = f(\dot{\varepsilon})$ has the form of a power function.

The energy of post-critical strain W_2 of a sample depends on strain rate. The statistical analysis has shown the monotonous growth of the parameter with the increasing strain rate, according to the linear regression function for conglomerates, and power regression function for the remaining rock types.

For the analysed rock groups, the statistical analysis has indicated a relation between the total strain energy W and the strain rate of the rock sample. The dependence $W = f(\dot{\varepsilon})$ was approximated by a power function, and the dependence $W = f(\log \dot{\varepsilon})$ — by a linear function.

Kinetic energy E_k determines the character of rock sample failure. A violent failure of a sample is caused by the positive kinetic energy, i.e. energy of elastic strain A_{el} must be sufficiently higher than strain energy in the post-critical part of the stress-strain characteristic. Most of the analysed rock samples undergo rapid failure as the calculated kinetic energy has a considerable positive value.

Similar to other parameters, the value of kinetic energy has been analysed as a function of strain rate. This dependence can be approximated by a linear or power function. The dependence of kinetic energy on strain rate is most evident for conglomerates, sandstones and coals.

6. Analysis of indexes of rock susceptibility to bumps in relation to strain rate

From among indexes of rock susceptibility to bumps, the index of dynamic failure λ , index of potential elastic energy PES and index of bump softening W_{OT} depend on strain rate (Bukowska, Krzysztoń, 1996). The remaining indexes, determined from strain parameters and specific energies, defined on the basis of the pre-critical part of the stress-strain characteristic, i.e. index of potential bumping K , energy index of rock susceptibility to bumps at strength limit W_{ET} , and index of bump hazard W_{ZT} do not depend on strain rate in the range 10^{-4} to 10^{-1} s^{-1} .

The index of potential bumping K does not change monotonously with the increasing strain rate. The values of this index exceed 0.7 (70%) for the analysed rocks in the Upper Silesian Coal Basin, which classifies the rocks as susceptible to bumps.

The energy index of rock susceptibility to bumps at strength limit W_{ET} encompasses greater amount of non-reversible strain energy than the conventional index. This energy also embraces permanent strains caused by microfailures of the rock structure in the pre-critical phase, appearing for stresses close to the instantaneous strength. Although, the elastic energy increases with the increasing strain rate, the energy index of bumping at strength limit is not a monotonous function. This is due to the irregular changes of non-reversible strains. The index W_{ET} assumes highest values for dull coal, and lowest for medium-grain sandstone.

The index of bump hazard W_{ZT} for all the analysed rocks is much lower than unity — value characteristic of brittle rock failure. The closer the index to unity, the more violent is the rock failure (Gustkiewicz et al., 1987).

The index of potential elastic energy PES significantly depends on strain rate in the range 10^{-4} to 10^{-1} s^{-1} (Fig. 5.6). This dependence has a character of a power regression with positive correlation coefficients.

The influence of strain rate on the index of dynamic failure λ has been observed for mudstones, siltstones and semi-bright coals. These are power relations with negative correlation coefficients. In other cases (conglomerates, sandstones, dull coals) no such an influence of strain rate within the range of 10^{-4} to 10^{-1} s^{-1} has been observed. For waste rock of the Upper Silesian Coal Basin the index assumes values 3 to 6, which is indicative of violent rock failure hazard. The index of dynamic failure assumes higher values for coals ranging between 6.94 and 13.93.

The influence of strain rate on the index of bumping softening W_{OT} is weaker than in the two above mentioned cases. It can be observed for mudstones and coals. No influence of strain rate on the analysed index has been observed for the remaining rocks.

6.1. Histograms of indexes of rock susceptibility to bumps

It follows from the investigations that only 3 indexes of rock susceptibility to bumps depend on strain rate. They are: index of potential elastic energy PES , index of dynamic failure λ and index of bump softening W_{OT} . Yet, the dependence of these indexes on strain rate does not hold for all lithological rock types. To illustrate the appearing dependences, histograms have been presented to show the values of individual indexes for the strain rates used in the analyses.

The potential elastic energy increases with the growing strain rate for all analysed lithological rock types. In the case of sandstone and coals PES varies from colliery to colliery (Fig. 6.1 a); on the other hand, conglomerates, mudstones and siltstones change in the same manner, regardless the sampling site in the individual mines and lithostratigraphic horizons (Fig. 6.1 b).

The index of dynamic failure decreases with the growing strain rate for coals, mudstones and siltstones, provided the dependences are the same for all samples representing the same lithological rock type (Fig. 6.2). No dependence has been observed for conglomerates and sandstones.

The index of bump softening depends on strain rate only for mudstones and coals in the same way for the whole lithological rock type (Fig. 6.3).

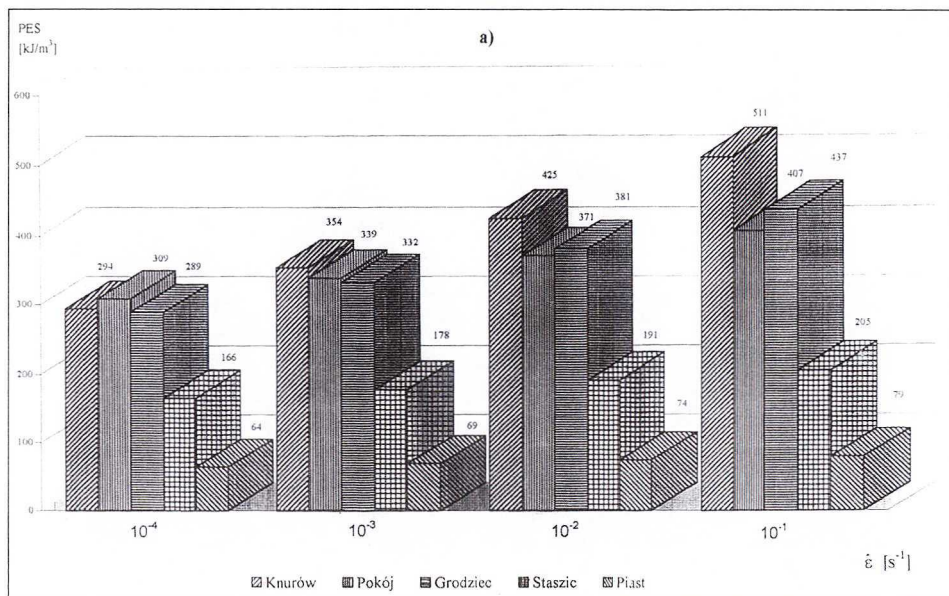


Fig. 6.1. Histogram of changes of potential elastic energy with strain rates a) for sandstones

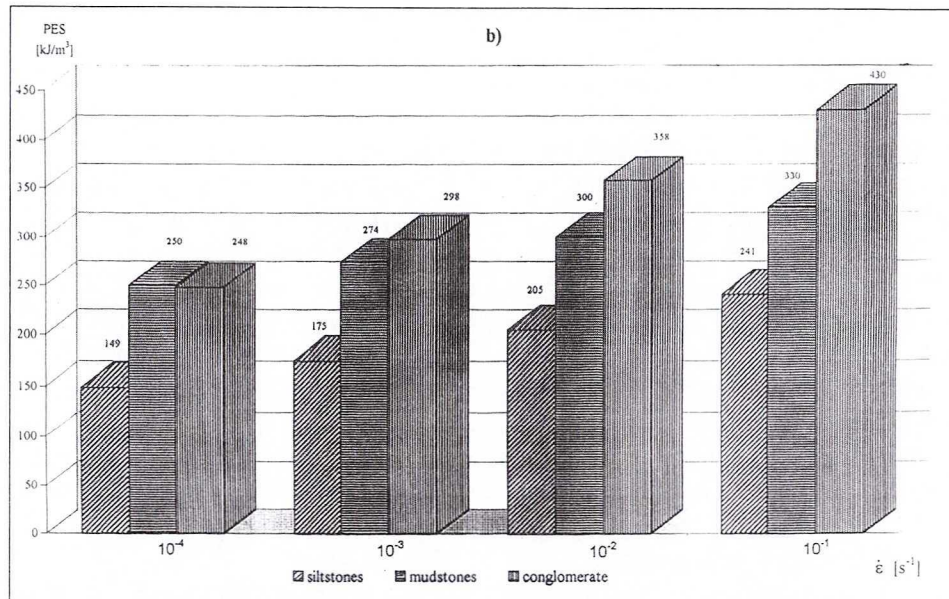


Fig. 6.1. Histogram of changes of potential elastic energy with strain rates b) for siltstones, mudstones and conglomerate

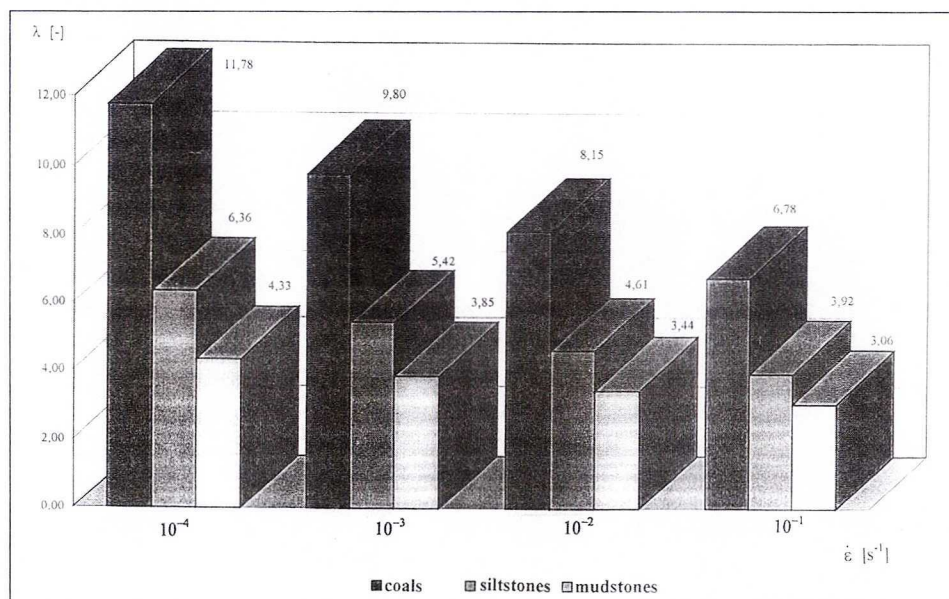


Fig. 6.2. Histogram of changes of the dynamic failure index with strain rates for coals, siltstones and mudstones

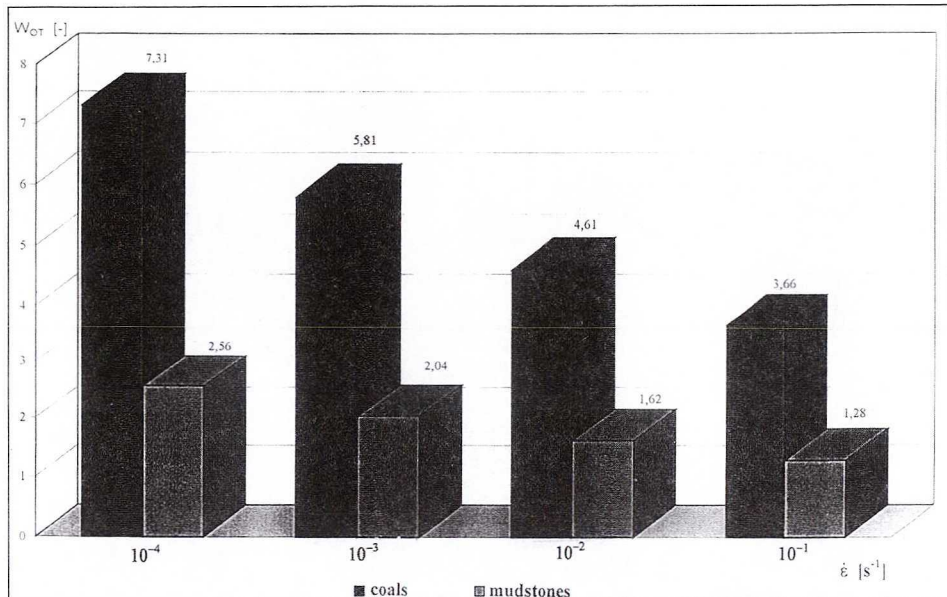


Fig. 6.3. Histogram of changes of the bump softening index with strain rates for coals and mudstones

7. Global presentation of investigation results

The investigations carried out have shown the influence of strain rate on the specific energies in the particular ranges of rock sample longitudinal strain and on the indexes of rock susceptibility to bumps.

For a global presentation of the obtained results, a three-dimensional laminar histogram has been designed where the particular specific energies and changes of their values with the strain rate increment have been shown. As an example, the histograms for coals (Fig. 7.1) and mudstones (Fig. 7.2) have been shown. The remaining rock types exhibit a similar kind of changes. The three-dimensional histograms illustrate not only the influence of strain rate on the investigated energies but also present the relative values of particular energies in relation to the total energy.

The large participation of the elastic energy A_{el} , in the total strain energy W and comparatively small amount of the post-critical strain energy W_2 can be observed in the graphs. The recoverable strain energy W_3 , dependent on the residual stress, has an insignificant value and in further considerations may be neglected. The kinetic energy E_k and the energy of non-reversible strain in the pre-critical part A_n do not show monotonous changes with the strain rates increase.

The indexes of susceptibility to bumps, dependent on rock strain rates, for coals (Fig. 7.3) and mudstones (Fig. 7.4) have been presented in analogous histograms. The numerical values of particular indexes can be read from histograms with regard to

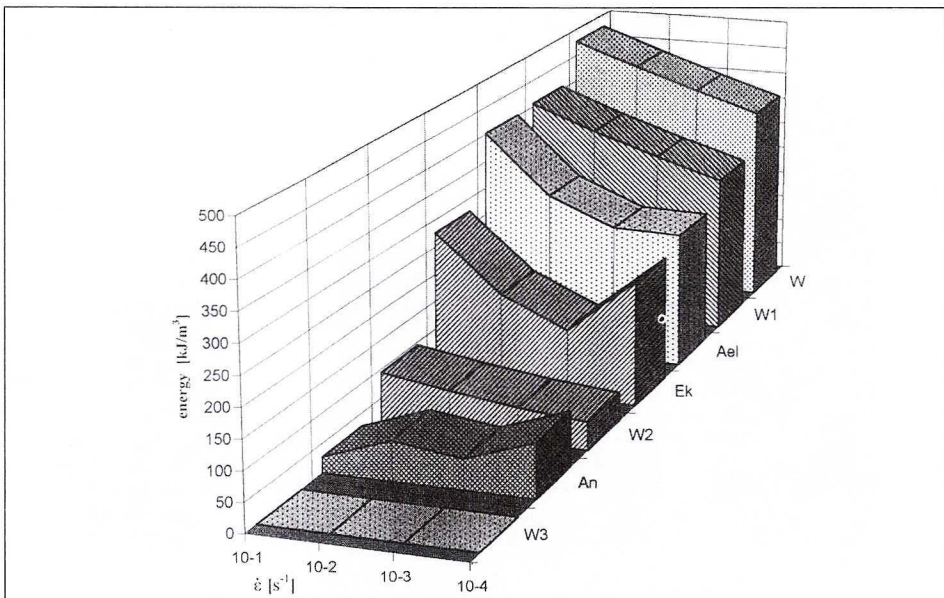


Fig. 7.1. Energies of longitudinal strain in dependence on the strain rate for coals (seam 507/510 — colliery "Rozbark")

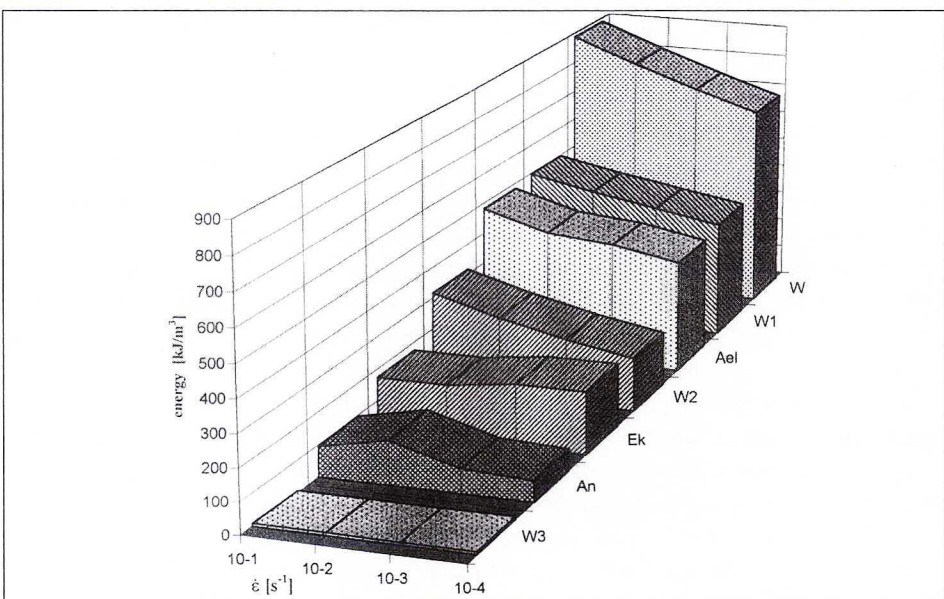


Fig. 7.2. Energies of longitudinal strain in dependence on the strain rate for mudstones (roof of seam 713/1—2 — colliery "Anna")

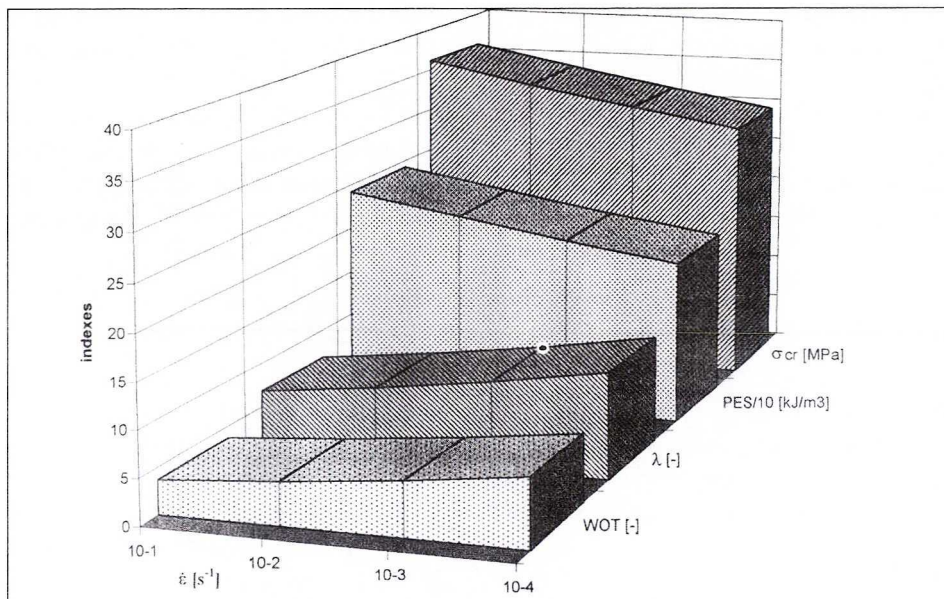


Fig. 7.3. Indexes of susceptibility to bumps for coals

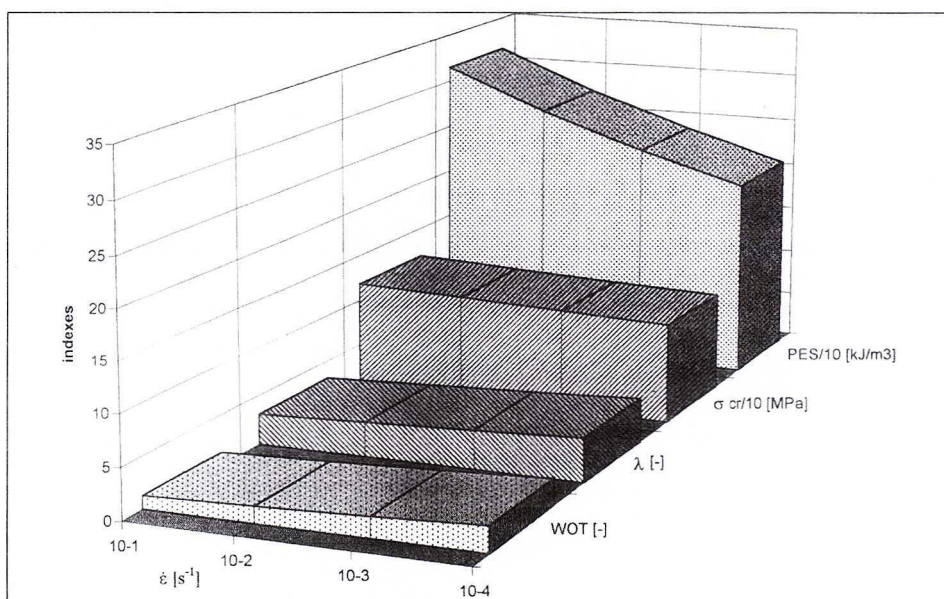


Fig. 7.4. Indexes of susceptibility to bumps for mudstone

the introduced scale. The indexes σ_{cr} and PES increase distinctly, although the indexes λ and W_{OT} decrease with the strain rate increment; however the rate of changes of the individual indexes depends on the rock type (Figs. 7.3 and 7.4).

The index of bump softening W_{OT} determined as the elastic energy to post-critical strain energy ratio (A_{el}/W_2) reveals the same tendency of changes as the index of dynamic failure expressed by the drop modulus to the elasticity modulus ratio (M/E). The reason of this is that when the area of the post-critical surface W_2 decreases, the drop modulus M assumes a greater value.

8. Applicability of the obtained results in the mining practice

In the extensive definition of the notion of “*bump*”, given by the International Bureau of Strata Mechanics, the fundamental reasons causing bumps are taken into consideration, namely: the critical state of stress of a part of a coal seam adjoining to mining workings, the elastic energy of a coal seam (rock) in the focus of burst and the energy of the surrounding rocks as well as the rate of energy release exceeding the rate of energy dissipated in a consequence of the non-reversible strains. Some of these reasons producing bumps may be analysed on the basis of investigations carried out in a stiff testing machine which may be treated as analogous to the *roof-seam-floor* system.

In the Upper Silesian Coal Basin the floor has the higher strength-deformation parameters than the seam, hence the stiffness of the basis may be assumed to be constant and then the consideration may be limited to the seam-roof system. Two extreme cases of *strong roof and weak seam* or of *weak roof and strong seam* may be considered.

In the case of a *strong roof*, the *weak seam* deforms under the influence of overburden rocks, and because of the low value of critical stress, particular parts of the seam undergo failure. The modulus of elasticity of sandstone, occurring immediately at the roof, is considerably greater than the drop modulus of coal undergoing failure ($E_{roof} > M_{coal}$) (Table 2).

TABLE 2

Strong roof-weak coal seam system in the colliery “Knurów” (seam 402/2) as an example of steady seam failure (strain rate $10^{-4}, \text{s}^{-1}$)

Rock	Critical stress [MPa]	Modulus of elasticity [MPa]	Drop modulus [MPa]	Potential elastic energy [kJ/m ³]	Kinetic energy [kJ/m ³]	Specific energy of longitudinal strain [kJ/m ³]
sandstone	79.3	9256	39148	340	142	563
coal	17.4	1689	4510	90	27	193

Then the stable destruction of seams occurs. In the case of roof caving, the situation in a mining working may be treating with regard to the possibility to the discharge

of a great value of the elastic energy accumulated in the strong roof. In such conditions the prevention measures should be undertaken in the seam roof.

In the second case of a weak roof and a strong seam, the elastic modulus of roof is smaller than the drop modulus of seam ($E_{\text{roof}} < M_{\text{coal}}$) and the seam-roof system works as a rock sample compressed in a soft testing machine (Table 3).

TABLE 3

Weak roof-strong coal seam system in the colliery "Niwka-Modrzejów" (seam 510) as an example of dynamic seam failure (strain rate $10^{-4}, \text{s}^{-1}$)

Rock	Critical stress [MPa]	Modulus of elasticity [MPa]	Drop modulus [MPa]	Potential elastic energy [kJ/m ³]	Kinetic energy [kJ/m ³]	Specific energy of longitudinal strain [kJ/m ³]
conglomerate	67.7	7500	55886	305	213	443
coal	42.9	2846	40156	320	440	595

After exceeding the coal strength, the dynamic effect caused by the violent discharge of the energy accumulated in a roof occurs. *The bump hazard can be reduced by prevention measures introduced to the seam, i.e. current discharge of the accumulated elastic energy by ratios which do not cause the bump hazard.*

Rock strain rates are an important factor in the considered cases, because the values of potential elastic energy increase considerably with the strain rates increment which, as a result, causes a greater hazard of dynamic phenomena occurrence.

9. Conclusions

1. It follows from the analyses that stress, strain and energy (specific energy) parameters as well as indexes of rock susceptibility to bumps depend to a varying degree on strain rate. These dependences assume the form of power or linear functions.

2. The statistical analysis has shown that only some parameters depend on strain rate for all types of Carboniferous rocks. Among parameters influencing the potential bump hazard are: critical stress σ_{cr} (momentous strength to compression), potential elastic energy PES and energy of total longitudinal strain W .

3. The indexes of rock susceptibility to bumps, determined both from the pre- and post-critical part of the stress-strain characteristic, depend on the strain rate for only some rock types. The index of dynamic failure ($\lambda = M/E$) decreases with the strain rate of mudstones, siltstones and semi-bright coals. The index of bump softening ($W_{OT} = A_{el}/W_2$) shows the same tendency of changes for mudstones, semi-bright and dull coals.

4. The strain rate increments have an influence both on the increase in the critical stress and potential elastic energy as well as on the decrease in the indexes of dynamic rock failure and bump softening. This means that at greater strain rates the coal seam (pillar) will have a greater strength, after exceeding of which the smaller dynamic effect will appear than in the case of smaller strain rates. However, the destruction of a seam (pillar) part may cause a discharge of a great amount of elastic energy accumulated in the overburden rocks.

5. The influence of strain rate on the reduction of bump hazard should be analysed for specific cases of strength of coals and the neighbouring rocks, e.g.

a) for *strong roof* and *weak seam* we have a static failure of the seam ($E_{\text{roof}} > M_{\text{coal}}$). In the case of roof caving, there exists a possibility of a discharge of great energy accumulated in a strong roof.

b) for *weak roof* and *strong seam* the seam-roof system behaves as a rock sample compressed in a soft test machine ($E_{\text{roof}} < M_{\text{coal}}$). After the coal strength is exceeded, the dynamic effect is simultaneously reinforced by the discharge of elastic energy accumulated in the roof.

6. The prevention of bumps requires the analysis of particular cases of the seam-roof system and the application of a suitable control of the advance front rate which has an influence on rock strain rates as well as the control of the roof of a seam, the accumulated energy of which should be decreased by the forced bumps or roof rocks wetting.

REFERENCES

- Bich J., 1962. Determination of dynamic hazards of coal seams (in Russian). Trudy WNIMI, sb. 49, Leningrad.
- Bieniowski Z. T., 1970. Time-dependent behaviour of fractural rock. Rock Mechanics, v. 2, No. 3, pp. 123—137.
- Bukowska M., 1994. The influence of strain rates on strength deformation properties of Carboniferous rocks of the Upper Silesian Coal Basin (in Polish). Sympozjum Nauk. Tech. Tąpania '94 pt. Rozwiązania inżynierskie w problematyce tąpań, pp. 11—18, Ustroń 1994.
- Bukowska M., 1996. Wpływ prędkości odkształcenia skał na wskaźniki skłonności skał do tąpań. Praca doktorska, Główny Instytut Górnictwa, Katowice.
- Filcek H., 1986. Rola pozniszczeniowej charakterystyki naprężeniowo-odkształceniowej skał w zagadnieniu tąpań. Kwartalnik AGH, seria: Górnictwo, z. 2, Kraków, 177—184.
- Gustkiewicz J., 1987. Wpływ wody na mechaniczne własności skał tąpiących. Sprawozdanie etapowe. Instytut Mechaniki Górotworu PAN, Kraków 1987.
- Heasley K. A., 1991. An examination of energy calculations applied to coal bump prediction. Rock Mechanics as a Multidisciplinary Science. Balkema, pp. 481—490, Rotterdam.
- Krzysztoń D., 1989. Pre- and post-failure stress-strain characteristics of dry and wet sandstone samples. Proceedings of the 2nd International Conference on Mining and Metallurgical Engineering, Suez Canal University, v. 1, pp. 120—149, Suez-Egypt.
- Krzysztoń D., 1989. Badanie energii odkształcenia podłużnego suchych i mokrych próbek piaskowca. Zeszyty Naukowe AGH, seria: Górnictwo, z. 145, Kraków, 215—230.
- Krzysztoń D., 1992. Energy analysis during compression tests of rock samples. Proceedings of the 12th Session of the International Bureau of Strata Mechanics, Leeds, 8—13 July, Balkema, 85—93.

- Krzysztoń D., Sanetra U., 1994. Analiza parametrów określających skłonność skał do tąpań. Sympozjum Nauk-Techn. Tąpania '94 pt. Rozwiązania inżynierskie w problematyce tąpań. Ustroń, 29–36.
- Majcherczyk T., 1989. Badanie fizycznych własności skał. Skrypty Uczelniane AGH nr 1175, Kraków.
- Minh V. C., 1989. Energy Analysis of Deformation and Failure of Rocks. Rozprawa habilitacyjna. Wydział Geologii UW, Warszawa.
- Peng S. S., 1973. Time-dependent aspects of rock behaviour as measured by servo-controlled hydraulic testing machine. *Int. J. Rock Mech. Min. Sci.* No. 3.
- Smolka J., 1978. Metoda określania skłonności do tąpań zwięzłych piaskowców i łupków piaszczystych (mułowców) otaczających pokłady węglowe. Praca nie publikowana Nr 010061434, GIG, Katowice.
- Wawersik W. R., Fairhurst C., 1970. A study of brittle rock fracture in laboratory compression experiments. *Int. J. Rock Mech. Min. Sci.* No. 6, v. 7, pp. 561–575.

REVIEW BY: PROF. DR HAB. INŻ. DANUTA KRZYSZTOŃ, KRAKÓW

Received: 27 October 1999.